Accumulating ammoniacal nitrogen instead of melanoidins determines the anaerobic digestibility of thermally hydrolyzed waste activated sludge

Pavez-Jara, Javier A.; van Lier, Jules B.; de Kreuk, Merle K.

DOI
10.1016/j.chemosphere.2023.138896

Publication date
2023

Document Version
Final published version

Published in
Chemosphere

Chemosphere 332 (2023) 138896

Contents lists available at ScienceDirect

Chemosphere

journal homepage: www.elsevier.com/locate/chemosphere

Accumulating ammoniacal nitrogen instead of melanoidins determines the anaerobic digestibility of thermally hydrolyzed waste activated sludge

Javier A. Pavez-Jara *, Jules B. van Lier, Merle K. de Kreuk

Department of Water Management, Delft University of Technology, Building 23 Stevinweg 1, 2628, Delft, The Netherlands

HIGHLIGHTS

- Thermal hydrolysis process (THP) of waste activated sludge produced partially biodegradable melanoidins.
- Ammoniacal nitrogen was limitedly released during THP.
- Ammoniacal nitrogen increased drastically during subsequent digestion of THP sludge.
- 20 gCOD/L melanoidins did not acutely inhibit full-scale acetotrophic methanogens.
- Free ammoniacal nitrogen inhibited acetotrophic methanogenesis in THP sludge digestion.

GRAPHICAL ABSTRACT

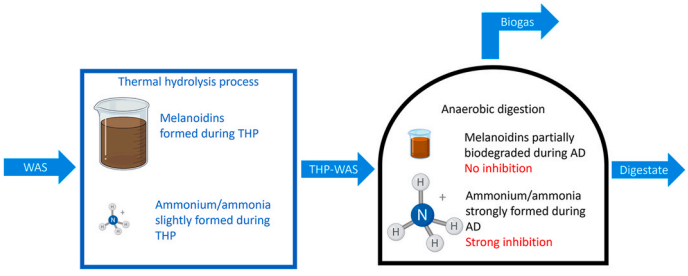

ARTICLE INFO

Handling Editor: A Adalberto Noyola

Keywords:
Pre-treatment
Thermal hydrolysis process
Ammonium release
Inhibition
Anaerobic digestion
Melanoidins

ABSTRACT

Full-scale thermal hydrolysis processes (THP) showed an increase in nutrients release and formation of melanoidins, which are considered to negatively impact methanogenesis during mesophilic anaerobic digestion (AD). In this research, fractionation of THP-sludge was performed to elucidate the distribution of nutrients and the formed melanoidins over the liquid and solid sludge matrix. Degradation of the different fractions in subsequent AD was assessed, and the results were compared with non-pre-treated waste activated sludge (WAS). Results showed that the THP-formed soluble melanoidins were partially biodegradable under AD, especially the fraction with molecular weight under 1.1 kDa, which was related to protein-like substances. The use of THP in WAS increased the non-biodegradable soluble chemical oxygen demand (sCOD) after AD, from 1.1% to 4.9% of the total COD. The total ammoniacal nitrogen (TAN) concentration only slightly increased during THP without AD. However, after AD, TAN released was 34% higher in the THP-treated WAS compared to non-treated WAS, i.e., 36.7 ± 0.7 compared to 27.4 ± 0.4 mgTANreleased/gCODsubstrate, respectively. Results from modified specific methanogenic activities (mSMAs) tests showed that the organics solubilised during THP, were not inhibitory for acetotrophic methanogens. However, after AD of THP-treated sludge and WAS, the mSMA showed that all

Abbreviations: +AD, samples taken after the BMP was performed; AD, anaerobic digestion; AMPTS, automated methane potential test system; BMP, biochemical methane potential; BSA, bovine serum albumin; EBPR, enhanced biological phosphorus removal; EPS, extracellular polymeric substances; FAN, free ammonia nitrogen; FEEM, Fluorescence excitation emission matrix; mSMA, modified specific methanogenic activity; MW, molecular weight; NFRI, normalised fluorescence regional integration; sCOD, soluble chemical oxygen demand; SDOS, specific degree of solubilisation; SEC-HPLC, size exclusion chromatography; SMA, specific methanogenic activity; TAN, total ammoniacal nitrogen; tCOD, total chemical oxygen demand; THP, thermal hydrolysis process; THP_l, THP-liquid; THP_s, THP-solid; THP_t, THP-total; TS, total solids; UFLC, ultrafast liquid chromatography; URI, ultraviolet absorbance ratio index; UVA 254, ultraviolet absorbance at 254 nm; VFA, volatile fatty acids; VS, volatile solids; WAS, waste activated sludge; WWTP, wastewater treatment plant.

* Corresponding author.
E-mail addresses: j.a.pavezjara@tudelft.nl (J.A. Pavez-Jara), j.b.vanlier@tudelft.nl (J.B. van Lier), m.k.dekreuk@tudelft.nl (M.K. de Kreuk).

https://doi.org/10.1016/j.chemosphere.2023.138896
Received 7 December 2022; Received in revised form 4 May 2023; Accepted 7 May 2023
Available online 9 May 2023

analysed samples presented strong inhibition on methanogenesis due to the presence of TAN and associated free ammonia nitrogen (FAN). In specific methanogenic activities (SMAs) tests with incremental concentration of TAN/FAN and melanoidins, TAN/FAN induced strong inhibition on methanogens, halving the SMA at around 2.5 gTAN/L and 100 mgFAN/L. Conversely, melanoidins did not show inhibition on the methanogens. Our present results revealed that when applying THP-AD in full-scale, the increase in TAN/FAN remarkably had a greater impact on AD than the formation of melanoidins.

1. Introduction

One of the most critical challenges for wastewater treatment facilities in many countries is the handling and disposal of waste activated sludge (WAS) (Fytili and Zabaniotou, 2008; Kelessidis and Stasinakis, 2012; Yang et al., 2015). Among possibilities to stabilise WAS, anaerobic digestion (AD) is a well-established technology since it has shown, high system robustness, reduction of pathogens, and recovery of the biochemical energy as biogas (Lin et al., 1997; Appels et al., 2008). However, the conversion efficiency of organics present in WAS into biogas in a conventional AD process is still low, ranging between 20 and 50% (Kabouris et al., 2009; Luostarinen et al., 2009; Ohemeng-Ntiamoah and Datta, 2018). To improve the bioconversion rate and CH_4 yield, different pre-treatments for organic substrates have been proposed such as mechanical, thermal, chemical, and biological techniques, or integrations of these (Zhen et al., 2017; Gonzalez et al., 2018). Whitin full-scale installations using pre-treatment processes for WAS digestion, thermal hydrolysis process (THP) is a commonly applied technology, which is offered by different companies. Some THP brand names present in the market are Cambi®, Biothelys®, Exelys®, THP®, LysoTherm® and Turbotec®. THP suppliers claim to improve biogas production, dewaterability, and to reach a pathogens-free digestate (Kepp et al., 2000; Pérez-Elvira et al., 2010). THP follows a sequence of two steps. The first step consists of heating the product to be hydrolyzed which may consist of secondary sludge, primary sludge or a mix of both, up to 140–180 °C (at 4–10 bar) for a determined time. Commonly, 20–40 min is set by the manufacturer. In the second step, the pressure is suddenly released, causing the pressurised-hot-water in the microbial biomass to evaporate, producing a violent expansion with the subsequent lysis, and release of the cytoplasmic content (Ringoot et al., 2012).

Despite the advantages of THP, several authors have reported the potential formation of recalcitrant and even inhibitory or toxic compounds due to the occurrence of side reactions during this process (Haug et al., 1978; Valo et al., 2004; Barber, 2016). The formation of recalcitrant and/or inhibitory compounds is reported to increase along with the THP pre-treatment time and temperature in the majority of the cases (Dwyer et al., 2008). Although different studies have found inconclusive results about the specific cause of possible inhibition of AD caused by THP, negative effects might be attributed to intermediates of Maillard and caramelisation reactions that are formed during the THP process (Penaud et al., 2000; Higgins et al., 2017; Ortega-Martínez et al., 2021; Balasundaram et al., 2022; Rahmani et al., 2023). Melanoidins can be formed during THP since organic compounds in WAS mainly consist of proteins, carbohydrates, and small portions of lipids and humic substances (Wilén et al., 2003; Gonzalez et al., 2018), which react during THP in caramelisation and Maillard reactions. During the Maillard reaction, an amino group present in amino acids/peptides/proteins reacts with the “glycosidic” hydroxyl group present in sugars to produce an Amadori-rearrangement-product, which is a Maillard reaction precursor (Ellis, 1959). If the conditions are favourable, the products of the initial rearrangements continue reacting, leading to the formation of intermediates that suffer polymerization reactions, and will thus increase in molecular weight (MW). The reaction products will form a wide range of compounds called melanoidins (Hodge, 1953; Horvat and Jakas, 2004; Silván et al., 2006). Since the structure of melanoidins is not well defined and the environmental conditions can modify them, melanoidins refer to a group of molecules that behave similarly instead of to one specific compound. Melanoidins can be classified based on MW and solubility, in a similar way as the classification of humic substances in humic and fulvic acids and humins (Migo et al., 1993; Klavins et al., 1999). In literature, it is hypothesised that melanoidins might cause inhibition of the anaerobic process (Chandra et al., 2008). However, the extent of this inhibition or the factors affecting inhibition are not fully understood (Brons et al., 1985; Rufian-Henares and de la Cueva, 2009; Li et al., 2019; Yin et al., 2019; Gao et al., 2022; Wang et al., 2022).

Besides the solubilisation of organics during THP, an increased nutrients release has also been observed (Suárez-Iglesias et al., 2017; Ngo et al., 2021). This (extra) solubilisation may cause operational problems in the subsequent steps of the reject water or sludge treatment. Additional maintenance may be required because of uncontrolled NH_4^+-PO_4^{3-}-based minerals precipitation that causes pipe clogging or problems in the sludge dewatering installation. Furthermore, additional total ammoniacal nitrogen (TAN = NH_4^++NH_3) release could lead to NH_4^+ and free ammonia nitrogen (FAN) inhibition of methanogenesis. The inhibition is mainly caused by FAN but the influence of TAN cannot be isolated (Astals et al., 2018). TAN/FAN are formed due to the breakdown of proteinaceous material (deamination) during AD and can cause inhibition of the process, especially in substrates with low C/N ratio (Wilson and Novak, 2009; Mata-Alvarez et al., 2014; Barber, 2016; Akindele and Sartaj, 2018). An elevated concentration of TAN/FAN may lead to an increased pH of the reactors since the pKa of $NH_4^+/NH_3 = 8.9$ at 35 °C. Moreover, TAN/FAN exert a higher degree of inhibition on acetoclastic methanogens than hydrogenotrophic methanogens (Koster and Lettinga, 1984). The somewhat higher pH and temperature in AD reactors using THP as pre-treatment, i.e. around 40 °C according to Barber (2016), increases the FAN concentration and thus the potential inhibition. In addition to this inhibitory effect, high TAN concentrations might lead to an increase in the costs of reject water deammonification, either via nitrification/denitrification, partial nitritation/anammox, or physicochemical techniques (Fux and Siegrist, 2004; Vineyard et al., 2020; Deng et al., 2021; Ochs et al., 2023), since the costs are proportional to the mass of TAN to be removed.

In our present study, the formation of recalcitrant compounds and the release of N from the different fractions of THP sludge and WAS monitored, and their effect on AD was determined. The distribution of melanoidins and N between supernatants and sludge pellets of centrifuged THP sludge was studied and compared to WAS without pre-treatment to elucidate the origin and fate of N and melanoidins. An evaluation of the melanoidins’ MW, aromaticity, and anaerobic biodegradability was also conducted, to determine their recalcitrant character. In addition, acetotrophic toxicity tests were performed to assess the possible inhibition of the THP-generated compounds on methanogenesis.

2. Materials and methods

2.1. Fractionation and characterisation of the substrates used for AD

Thickened WAS and THP-treated-WAS were collected immediately before and after a CAMBI® system from a municipal wastewater treatment plant (WWTP) located in Hengelo, The Netherlands. The sampling volume was 10 L, and only one sample of each sludge was taken. The WAS sample originated in an aerobic activated-sludge plant using enhanced biological phosphorus removal (EBPR) and nitrification/

denitrification. THP sludge samples were collected after passing a CAMBI® installation, pre-treating only secondary sludge from the WWTP in Hengelo and surrounding small WWTPs. The CAMBI® installation comprised a pulper to pre-heat the sludge, a reactor with an operational temperature of 160 °C and a treatment time per batch of 30 min, and a flash tank to perform the "steam explosion". The samples were stored at 4 °C before analysis and fractionation.

THP sludge was homogenised and centrifuged at 12,000 rpm for 10 min in a centrifuge model Sorvall ST 16 R (Thermo Fisher Scientific, USA) at 4 °C, whereafter the pellet and supernatant were collected. The pellet of THP sludge was washed three times in a culture medium consisting of buffer, macronutrients, and micronutrients (Table A1 in supplementary information), to remove the remnant soluble melanoidins. The washing was performed by doubling the pellet volume with culture medium and subsequently resuspending and centrifuging at 3500 rpm for 10 min in a centrifuge model Heraeus Labofuge 400 (Thermo Fisher Scientific, USA). Four different samples were analysed: i) THP-liquid (THP_l), comprising the centrifugation supernatant of THP sludge; ii) THP-solid (THP_s), consisting of the buffer-washed pellet of THP sludge; iii) THP-total (THP_t), comprising a homogenous sample of THP sludge; iv) WAS, comprising the non-pre-treated sample of thickened WAS. Note that THP_t and WAS were not processed by centrifugation and washing. For clarification, a scheme of the fractionation is included in the supplementary material (Figure A1).

2.2. Chemical analysis

Total solids (TS) and volatile solids (VS) were assessed according to Standard Methods for the examination of water and wastewater (Rice et al., 2012). Soluble and total chemical oxygen demand (sCOD and tCOD, respectively) and TAN, were measured with the kits LCK 114, APC 303, brand Hach Lange (Hach, USA). Carbohydrates were measured according to the phenol–sulphuric acid method (Dubois et al., 1951). Proteins and humic substances were measured based on the Lowry method considering the interference of humic substances, according to Fr et al. (1995). Volatile fatty acids (VFA) were measured using an Agilent 19091F-112, 25 m × 320 μm × 0.5 μm column in an Agilent 7890 A Gas Chromatograph (Agilent Technologies, USA) equipped with a flame ionisation detector. Helium was used as mobile phase with a total flow rate of 67 mL/min and a split ratio of 25:1, the sample injection volume was 1 μL. The gas chromatograph oven's temperature increased from 80 to 180 °C in 10.5 min, and the temperatures of the injector and detector were 80 and 240 °C, respectively. FAN was calculated in each sample based on equation (1), according to Emerson et al. (1975).

$$FAN = \frac{TAN}{\left(10^{pK_a - pH} + 1\right)} = \frac{TAN}{\left(10^{\frac{(0.901821 + 2729.92)}{T_k} - pH} + 1\right)} \quad (1)$$

Where.

TAN = TAN concentration ($NH_4^+ + NH_3$ in gN/L).
FAN= FAN concentration in gN/L.
pK_a = NH_4^+/NH_3 dissociation constant at the sample temperature (approximated as $pK_a = \frac{(0.901821 + 2729.92)}{T_k}$).
T_k = Sample temperature in K.

2.3. Biochemical methane potential (BMP) and modified acetotrophic specific methanogenic activity (mSMA) tests

BMP and mSMA tests were conducted with the four fractions formerly mentioned using an AMPTS II system (Bioprocess Control, Sweden) at 35 °C, considering the recommendations raised by Holliger et al. (2016). BMP tests were carried out in triplicate, using 500 mL bottles with a reaction volume of 300 mL. The BMP bottles comprising inoculum, substrate and culture medium were sampled for analysis at the beginning and the end of the AD. We obtained ten groups from the sampling: i) THP_l and THP_l + AD, comprising the THP_l substrate at the beginning and end of the BMP, respectively; ii) THP_s and THP_s + AD, comprising the THP_s substrate at the beginning and end of the BMP, respectively; iii) THP_t and THP_t + AD, comprising the THP_t substrate at the beginning and end of the BMP, respectively; iv) WAS and WAS + AD, comprising the WAS substrate at the beginning and end of the BMP, respectively; v) Blank and Blank + AD, comprising only inoculum and culture medium at the beginning and end of the BMP, respectively. The tests were conducted with a concentration of 19 g of tCOD per litre of substrate and 28.5 g of VS per litre of inoculum, having an inoculum/substrate ratio of 1.5 gVS/gCOD. In the blank bottles, the substrate was replaced by demineralized water, while the culture medium (Table A1 in supplementary information) and inoculum remained in the same concentration as in the tests with substrates. Results were expressed in millilitres of normalised CH_4 (273.15 K and 1 atm) produced per gram of substrate COD. The percentage of biodegradability of the analysed samples was assessed considering that 100% corresponded to 350 NmL-CH_4/gCOD.

The inoculum to perform the BMP and mSMA tests was collected from the digestate produced at municipal WWTP, Harnaschpolder operated by Delfluent Services (Den Hoorn, The Netherlands). These digesters treat a mixture of WAS and primary sludge without any pre-treatment, at a hydraulic retention time of 21–24 days and an operational temperature of 35 °C. In preparatory tests (results not shown), microcrystalline cellulose (Sigma-Aldrich, USA) was used as the substrate in positive controls with the inoculum from the same provenance, ensuring that the inoculum was active and produced the stoichiometric amount of CH_4 according to the added substrate. The inoculum was pre-incubated at 35 °C for seven days to consume the remaining substrate from the full-scale installation and was pre-concentrated 1.7 times by centrifugation 10 min at 3500 rpm in a centrifuge model Heraeus Labofuge 400 (Thermo Fisher Scientific, USA) to reach the required concentration to perform the experiments.

To study the differences in acetotrophic methanogenic activity of the inoculum before and after the BMP test, two mSMAs tests were conducted with the mixed broth used for BMP tests at the beginning and the end. The mSMA tests were conducted under the same conditions as the BMP tests, using the automated methane potential test system (AMPTS) II (Bioprocess Control, Sweden) at 35 °C, using the same culture media (Table A1 in supplementary information), and recording CH_4 generation over time. The mSMA tests were conducted using 2 gCOD/L of sodium acetate, which was added to the BMP-substrates THP_l, THP_s, THP_t, and WAS, using the same inoculum. The BMP-blank-bottle plus sodium acetate was considered as mSMA positive control in which no substrate for BMP was added. The reaction volume of mSMAs before and after the BMP test was 300 mL and 250 mL, respectively, since 50 mL of broths were taken for analysis once the BMP test was ended (symbolised in the figures as "+AD" samples). Both mSMAs were carried out in triplicate and the bars in the graphs represent the standard deviation. The results were expressed in grams of COD as CH_4 produced per gram of VS inoculum per day, at the maximum CH_4 production rate.

Additionally, SMA tests with different concentrations of TAN/FAN and melanoidins were carried out, using the same inoculum as in the BMP and mSMA tests, in 500 mL bottles with 300 mL of reaction volume, and adding the same concentration of acetate and culture medium used for mSMAs. TAN was supplied as NH_4Cl (CAS Number 12125-02-9, Sigma-Aldrich, USA). Resulting FAN concentrations were calculated according to equation (1) and plotted together with TAN. The pHs used to calculate FAN were measured at the beginning of the BMP test since it was close to the point when the maximum CH_4 rate was measured. At the end of the BMP test (day 23), the pH of the broth was measured again for the FAN calculation. Soluble melanoidins were prepared to resemble the humic substances formed during THP. Melanoidins were prepared according to Bernardo et al. (1997) and Dwyer et al. (2008): by reacting

0.25 M glucose and 0.25 M glycine using 0.5 M $NaHCO_3$ as buffer, for 3 h at 121 °C, in an autoclave model FVA3/A1 (Fedegari Autoklaven AG, Switzerland). After the incubation, the synthetic melanoidins solution was anaerobically digested at 35 °C using anaerobic inoculum in a proportion of 1 g $VS_{inoculum}$/g COD $_{melanoidins}$ in order to reduce the amount of readily-biodegradable organics, such as short molecular weight melanoidins and non-reacted glucose and glycine. After the gas production stopped, the digested melanoidins supernatant was separated from the digestate using centrifugation at 3500 rpm for 10 min in a centrifuge model Heraeus Labofuge 400 (Thermo Fisher Scientific, USA), characterised, and stored at 4 °C for further use. The inhibitory effect on SMA was modelled using equation (2), which is analogous to the equation used in ADM1 to model pH inhibition (Astals et al., 2018). Also, the half inhibition constant was calculated as $(KI_{min} + KI_{max})/2$.

$$SMA = \begin{cases} SMA_{i,max}, \text{if } [S_i] \leq KI_{min} \\ SMA_{i,max} \times e^{-2.77259 \times \left(\frac{([S_i]-KI_{min})}{(KI_{max}-KI_{min})}\right)^2}, \text{if } [S_i] \rangle KI_{min} \end{cases} \quad (2)$$

Where.

$SMA_{i,max}$ = SMA measured when inhibition starts.
$[S_i]$: inhibitor concentration (i = TAN and FAN).
KI_{max}: inhibitor concentration at which the inhibition is almost complete (assumed as SMA = 0.06· $SMA_{x,max}$).
KI_{min} = inhibitor concentration when inhibition starts.

2.4. Size exclusion chromatography (SEC-HPLC)

Employing SEC-HPLC we investigated the MW of the melanoidins formed during THP and their fate during AD. SEC-HPLC elutes the soluble molecules based on their hydrodynamic radius, which increases with the MW (Squire, 1985; Tarvers and Church, 1985). Absorbances at two wavelengths were used in the SEC-HPLC detector. One was measured at 254 nm, indicating the humic substances with a higher presence of phenolic groups (more condensed), and the other one was measured at 210 nm, which represented less condensed molecules associated with proteinaceous material (Her et al., 2008). Samples were taken before and after performing the BMP tests, filtered through 0.45 μm with a CHROMAFIL Xtra PES-45/25 (Macherey-Nagel, Germany), and analysed by SEC-HPLC using a column model Yarra™ 3 μm SEC-2000, LC Column 300 × 7.8 mm, Ea (Phenomenex, USA) connected to an ultrafast liquid chromatography (UFLC) system (Prominence, Shimadzu, Japan). Acetonitrile and sodium PO_4^{3-} buffer of 10 mM, pH 7, prepared in ultrapure water in a proportion of 25% and 75%, respectively, were used as mobile phase. The eluent flow was 0.25 mL/min, and the separation was reached within 1 h at 25 °C. A UV detector was used at 254 nm and 210 nm to identify the analytes. Four Polystyrene sulfonate standards (Polymer standard service, Germany) of 0.1, 1.1, 3.6, and 29.1 kDa were used to correlate the elution time with the MW. The results were expressed as the area under the curve of the detector signal (in mV) in the timeframe that corresponds to the known MW defined in the standards. The UV absorbance ratio index (URI) describes the specific aromaticity of the soluble substances measured in SEC-HPLC. A high URI indicates the occurrence of protein-like moieties associated with carboxylic and hydroxyl groups, while a low value indicates phenolic groups occurrence and thus, aromaticity (Her et al., 2008). URI was calculated as the quotient of the averaged absorbances at 210 nm over 254 nm, in each MW interval.

2.5. Fluorescence excitation emission matrix (FEEM)

FEEM was conducted using a FluoroMax-3 spectrofluorometer (HORIBA Jobin Yvon, Japan) with a 1 cm path-length quartz cuvette. The samples were filtered through 0.45 μm and diluted with ultrapure water to reach a concentration of 1 mgTOC/L. Emission and excitation spectra were analysed from 290 to 500 nm and 240–452 nm with 2 and 4 nm of interval, respectively. The Raman peaks were removed and the blank (ultrapure water) was subtracted. The integration of the fluorophores was performed based on the location of the maximum peak method, according to Dwyer and Lant (2008). The FEEM was divided into three areas to perform normalised fluorescence regional integration (NFRI), as follows: protein-like substances (3320 nm^2) comprised the polygon formed by the points (290 nm, 240 nm), (290 nm, 268 nm), (328 nm, 308 nm), (350 nm, 308 nm), and (350 nm, 240 nm); fulvic-like compounds (7104 nm^2) comprised the polygon formed by the points (352 nm, 240 nm), (500 nm, 240 nm), (500 nm, 288 nm), and (352 nm, 288 nm); and humic-like compounds (16,472 nm^2) comprised the polygon formed by the points (352 nm, 288 nm) (500 nm, 288 nm) (500 nm, 452 nm) (472 nm, 452 nm), and (352 nm, 332 nm). The NFRI results comprised the volume under the FEEM in arbitrary units (AU*nm^2) in the three polygons analysed (protein-like, fulvic-like, and humic-like substances), over the area of the specific polygon in nm^2 (Chen et al., 2003).

2.6. True colour and UVA 254

True colour and UVA 254 were measured in the soluble fraction after filtration using 0.45 μm syringe filters CHROMAFIL Xtra PES-45/25 (Macherey-Nagel, Germany). The true colour was measured at 475 nm using a Platinum–Cobalt colour reference solution (Hazen 500, Certipur® Merck, Germany) with a concentration of 500 mgPt-Co/L in a Genesys 10 S UV–Vis spectrophotometer (Thermo Scientific, USA) using 1 cm pathway plastic cuvettes. UVA 254 was measured in the same spectrophotometer as the true colour measurement, at 254 nm with 1 cm pathway quartz cuvettes. The results are expressed in mg Pt–Co/L and 1/cm in the case of true colour and UVA 254, respectively.

2.7. Analysis of results

The specific degree of solubilisation (SDOS) describes the solubilisation of specific compounds of interest (i-th compound) in a particular moment per unit of mass in the initial substrate (expressed as COD), and it is defined in equation (3). SDOS was calculated at the beginning and end of AD, discounting the Blank sample at the same moment. For assessing this parameter, the soluble concentration of specific compounds in the blank sample (no substrate added) was subtracted from the soluble concentration before and after AD, and this was divided by the tCOD concentration in the initial substrate. The results are expressed in the mass of the i-th compound solubilised per mass of tCOD in the initial substrate. For instance, a TAN-SDOS of 40 mgTAN/gCOD at the end of AD, means that this specific substrate released 40 mg of TAN per gram of COD in the substrate once AD was completed.

$$i - SDOS = \left.\frac{C_{i,j} - C_{i,Blank}}{tCOD_j}\right|_{t=0 \text{ and } t=23} \quad (3)$$

Where.

t = Digestion time in days (t = 0 is considered before AD, t = 23 after AD)
i − SDOS = Specific degree of solubilisation of the i-th parameter.
$C_{i,j}$ = Soluble concentration of the i-th parameter in the j-th sample.
$C_{i,Blank}$ = Soluble concentration of the i-th parameter blank sample (before and after AD, respectively).
$tCOD_j$ = Substrate tCOD concentration (homogenous) in the j-th sample, before AD (19 gCOD/L).
i = sCOD, T. colour, UVA 254, TAN, and soluble proteins.
j = THP_l, THP_s, THP_t, and WAS.

To better understand the effect of THP conditions on the biode-

gradability of proteins in relation to the biodegraded organic matter during AD, the $TAN_{released}/COD_{consumed}$ ratio was calculated in all analysed fractions (COD balance in Figure A2 of supplementary material). TAN released per unit of total COD consumed is defined in equation (4). This parameter shows the TAN released per unit of biodegradable COD in the analysed substrates.

$$TAN_{released} \Big/ COD_{Consumed} = \frac{\left(TAN - SDOS_{+AD,j}\right) - \left(TAN - SDOS_{-AD,j}\right)}{\left(\frac{\left(tCOD_{-AD,j} - tCOD_{-AD,Blank}\right) - \left(tCOD_{+AD,j} - tCOD_{+AD,Blank}\right)}{COD_j}\right)} \quad (4)$$

Where.

$TAN - SDOS_{+AD,j}$ = TAN-SDOS after AD in the j-th sample.
$TAN - SDOS_{-AD,j}$ = TAN-SDOS before AD in the j-th sample.
$tCOD_{+AD,j}$ = tCOD concentration after AD in the j-th sample ($tCOD_{+AD-Blank}$ = tCOD concentration in the Blank after AD).
$tCOD_{-AD,j}$ = tCOD concentration before AD in the j-th sample ($tCOD_{-AD,Blank}$ = tCOD concentration in the Blank before AD).

Single-factor ANOVA with a confidence level of 95% was used to evaluate the significance of differences between the different samples. Also, mean difference tests with the same level of significance as ANOVA were used when comparing two samples' averages.

3. Results and discussion

3.1. Fractionation of THP sludge samples

The biochemical parameters of WAS and the different fractions of THP sludge are given in Table 1. After fractionation, about 40% of the THP sludge (THP_t) consisted of THP_l, while 60% of the mass was found as THP_s. It is important to remark that the parameters measured in THP_l and THP_s corresponded to the concentrations reached after the fractionation that was performed in the laboratory and, therefore, do not represent values that can be found in a full-scale installation. The soluble biochemical parameters in the THP_l fraction were similar to those of the THP_t since both samples share the soluble portion of THP sludge. Measured VFAs in THP_l and THP_t could originate from the release of cytoplasmatic metabolites and/or physicochemical conversion of lipids, (long-chain) fatty acids and proteins present in WAS, which were solubilised. The increased TAN concentration in pre-treated samples was most likely produced by the physicochemical deamination of proteins during THP (Wilson and Novak, 2009). Melanoidins present in the THP sludge fractions caused the observed increase in UVA 254 and true colour compared to WAS. The percentage of solubilised organic matter after pre-treatment (sCOD/tCOD) increased from 0.5% in WAS to 32% in THP_t, evidencing the capacity of the pre-treatment to solubilise the organic compounds present in the WAS. The soluble compounds present in the THP_s fraction indicate that not all soluble substances were removed during the washing protocol, and some remained within the THP-treated sludge's solid matrix. In addition, true colour and UVA 254 were measured in the soluble phase only; the pre-treatment induced an increase of 650 and 300 times in true colour and UVA 254, respectively, compared to WAS. Elevated colour and UVA 254 during THP have been widely reported in the literature and have been attributed to the formation of melanoidins (Dwyer et al., 2008).

Table 1 also shows the BMPs of the analysed samples. Obtained values clearly indicate that the THP_l fraction had the highest biodegradability, reaching 66% of the theoretical CH_4 production. Furthermore, THP_s and WAS showed about 34% of biodegradability, indicating the low biodegradability of both substrates. The BMP of THP_t corresponded to the weighted average of the BMPs of THP_l and THP_s, given a mass distribution of 40% in the supernatant and 60% in the pellet during the fractionation. The assessed biodegradability of WAS and THP_t was slightly lower than the results obtained by Stuckey and McCarty (1984) and Jeong et al. (2019) at similar conditions. However, as suggested by Jeong et al. (2019), a high sludge concentration during THP may result in low BMP values of the pre-treated sludge due to mass transfer limitations. Notably, in our work, WAS pre-treated at a concentration of 16.6% (166.8 ± 0.4 gTS/L in Table 1), whereas in Jeong et al. (2019) the highest concentration reached was 7%. It is noteworthy that THP_t was sampled before it was diluted to enter the anaerobic reactors, which explains the high TS concentration. Moreover, in the case of WAS and THP_t the increment of about 35% in biodegradability (from 34% to 47%) due to pre-treatment is in accordance with the 25–27% increment that Jeong et al. (2019) found for mesophilic digestion after THP pre-treatment at 175 °C. On the other hand, Haug et al. (1978) showed a biodegradability of WAS between 32.5 and 42.5% and an increment of 22.2%, i.e., from 32.5 to 39.7% after pre-treatment. While the biodegradability in their work was similar, the attained increment was lower than the one obtained in our present work, even though pre-treatment conditions were similar (175 °C for 0.5 h).

Table 1
Biochemical parameters in the fractionation of THP sludge and WAS.

Measurement	THP_l fraction	THP_s fraction	THP_t sample	WAS sample
BMP (NmL-CH_4/gCOD) [% of biodegradability]	230 ± 23 [66 ± 7]	119 ± 35 [34 ± 10]	165 ± 24 [47 ± 7]	122 ± 22 [35 ± 6]
sCOD (g/L)	54.9 ± 0.9	9.76 ± 0.06	52.9 ± 0.2	0.95 ± 0.05
tCOD (g/L)	75 ± 2	238 ± 9	172 ± 1	212 ± 7
Total solids (gTS/L)	57.5 ± 0.1	187.3 ± 0.7	136.3 ± 0.5	166.8 ± 0.4
Volatile solids (gVS/L)	50.5 ± 0.4	131.1 ± 0.5	105.2 ± 0.1	130.6 ± 0.3
TAN (mg TAN/L)	1034 ± 8	389 ± 2	1068 ± 14	713 ± 12
Soluble proteins (mgBSA/L)	16,993 ± 1480	2406 ± 231	17,578 ± 896	Not detected.
Soluble carbohydrates (mg/L)	3353 ± 895	1025 ± 69	2488 ± 1053	367 ± 37
VFA (mgCOD/L)	1885 ± 81	210 ± 17	1997 ± 74	35.2 ± 0.2
UVA 254 (1/cm)	207.2 ± 0.2	41.93 ± 0.05	207.6 ± 0.2	0.688 ± 0.001
True colour (g Pt–Co/L)	81.0 ± 0.2	8.54 ± 0.02	84.1 ± 0.2	0.123 ± 0.002

3.2. Occurrence and degradation of melanoidins

Fig. 1-a shows the concentration of sCOD and its specific degree of solubilisation (sCOD-SDOS) in the studied samples before and after anaerobic digestion, ("+AD" indicates anaerobically digested samples). The sCOD-SDOS value relates the sCOD concentration at a specific moment to the initial substrate COD. This parameter is introduced to discount the effect of the culture medium, and inoculum due to endogenous respiration. Besides, the concentrations shown were measured in the reaction broth, which includes the substrate, inoculum, and culture medium. The sCOD-SDOS decreased after AD in all analysed samples, showing that organic matter, which was solubilised during THP, was largely biodegraded under anaerobic conditions. Results showed a very high anaerobic biodegradability of the sCOD observed in the samples THP_l and THP_t. On the other hand, THP_s and WAS showed less soluble organics before AD, which was a consequence of the particulate nature of the samples. The residual sCOD after AD was considered recalcitrant under anaerobic conditions, and accounted for 16.2, 1.4, 4.9 and 1.1% of the tCOD in THP_l, THP_s, THP_t, and WAS, respectively. In practice, anaerobically recalcitrant sCOD will leave the anaerobic digester with the reject water and will be conveyed to any subsequent step after AD, such as struvite precipitation and/or partial nitritation/anammox processes, or will be directed toward the WWTP headworks. The sCOD in the analysed samples was correlated with true

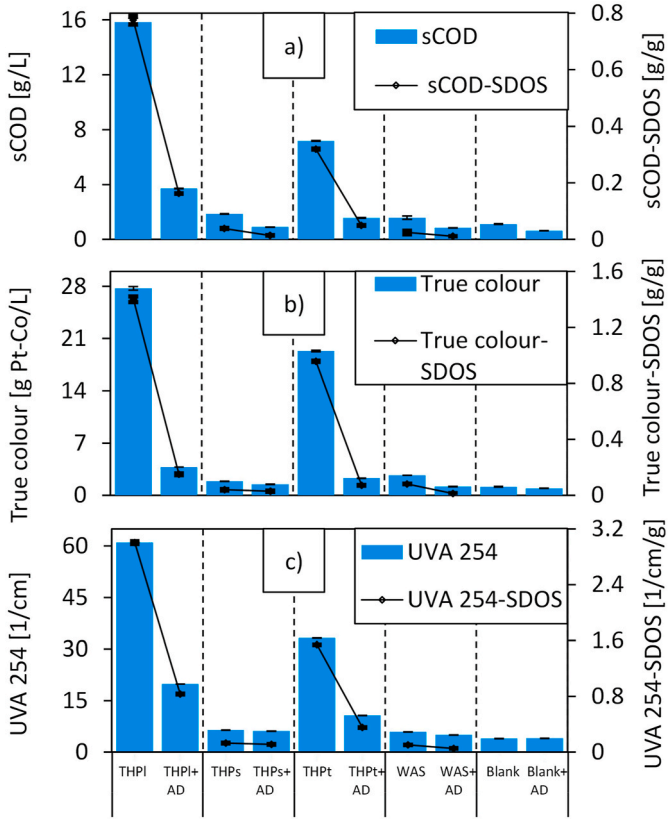

Fig. 1. Chemical analysis of the different THP-treated fractions and other sludge samples subjected to AD (indicated as + AD): a) Soluble COD concentration and sCOD-SDOS; b) True colour concentration and true colour-SDOS; c) UVA 254 concentration and UVA254-SCOD. The data consider the substrates dilution with inoculum and culture medium. (For interpretation of the references to colour in this figure legend, the reader is referred to the Web version of this article.)

colour (Fig. 1-b), UVA 254 (Fig. 1-c) and soluble proteins (Fig. 3-b), indicating that the solubilised organic matter contained proteins, aromatics, and coloured compounds such as melanoidins. The formation of soluble melanoidins in THP has been previously reported by Dwyer and Lant (2008), and colour and UVA 254 were used to estimate their concentration. Melanoidins, as well as humic substances, can be classified according to their acid/base solubility in i) fulvic acids (always soluble), ii) humic acids (insoluble at pH < 2) and iii) insoluble humins (Sutton and Sposito, 2005). However, in our present work, sCOD, true colour, and UVA 254 only accounted for the fulvic and humic fractions that are soluble at the pH of the experiments, without distinction between humic and fulvic acid fractions.

Fig. 2-a and Fig. 2-b show the MW distributions before and after AD as coloured bars in the soluble part of the analysed samples. The size of computed areas under the curve with 254 nm and 210 nm showed a similar trend as sCOD, true colour, UVA 254, and soluble proteins, in which THP_l followed by THP_t had the highest concentrations of humic substances, followed by THP_s and WAS. The concentration of humic substances (254 nm) decreased after AD. In addition, for both wavelengths, the MW of the humic substances before AD was mainly below 3.6 kDa, which according to MacCarthy (2001), corresponds to a fulvic acids fraction. The compounds measured in the Blank and WAS were very likely not melanoidins but extracellular polymeric substances (EPS), which are commonly present in aerobic and anaerobic biomass (Fr et al., 1995; D'Abzac et al., 2010). The presence of EPS-like compounds was more evident in WAS, in which the fraction larger than 29.1

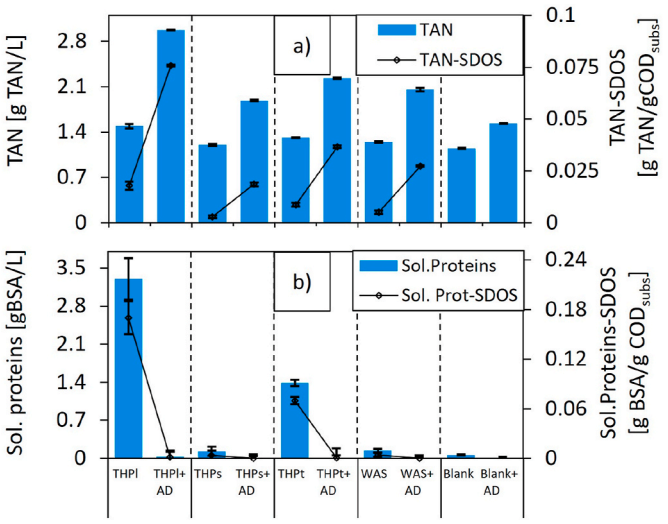

Fig. 3. a) TAN concentration and TAN-SDOS; b) Soluble proteins concentration and soluble proteins-SDOS; in the samples before and after (+AD) BMP tests, in the analysed samples.

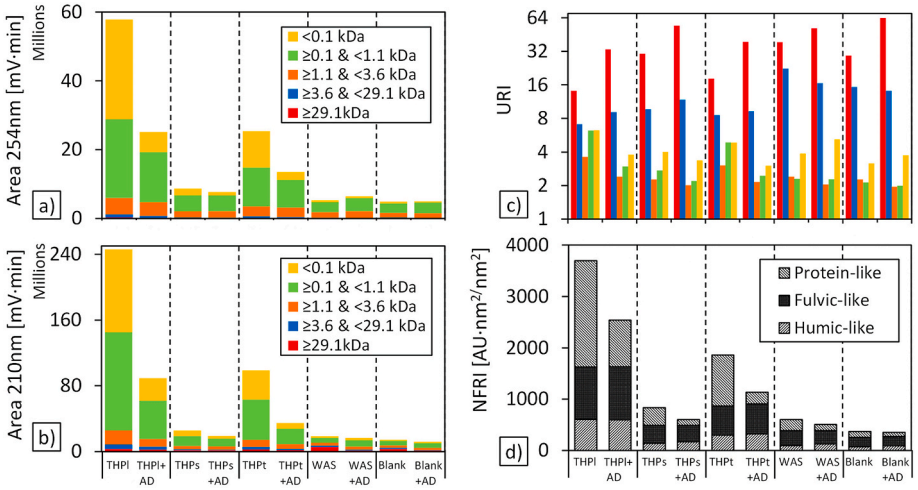

Fig. 2. a) Distribution of MWs at 254 nm; b) Distribution of MWs at 210 nm; c) URI in each MW interval (logarithmic scale); d) Protein-like, fulvic-like and humic-like NFRI in FEEM. Bars represent the samples before and after (+AD) anaerobic digestion.

kDa was the highest in the measurements at 210 nm (Fig. 2-b). After AD, the concentration of compounds measured at 254 nm and 210 nm decreased for all THP fractions, showing that the anaerobic microorganisms either consumed or adsorbed part of these substances, removing them from the soluble phase, as shown in Fig. 2-b and Fig. 2-c. For the pre-treated samples, the low MW molecules showed the highest biodegradability, and the fraction below 1.1 kDa, decreased in all samples analysed at 254 nm and 210 nm wavelengths. The low MW fraction may have consisted of furfural, hydroxymethylfurfural, and similar compounds, which have been identified as intermediates of Maillard reactions (Hodge, 1953). These compounds are reported to be biodegradable under anaerobic conditions (Boopathy, 2002; Park et al., 2012; Huang et al., 2019), which may explain our observed results (Fig. 2 -a and Fig. 2-b).

Fig. 2-c shows URI per range of MW in each of the samples analysed before and after AD. As can be observed in all fractionated THP samples, compounds with a MW exceeding 3.6 kDa increased the URI values during AD. This URI increase indicated that in these MWs ranges, either the microorganisms converted the aromatic compounds or there was an increase in the non-aromatic substances. Non-aromatic substances increase can possibly be attributed to the excretion of soluble EPS during anaerobic biomass growth in the batch reactors, increasing the UV210 absorbance in these fractions. Moreover, within the pre-treated samples, compounds with a MW below 3.6 kDa increased their aromaticity after AD, which is indicated by decreasing URI values. This indicates that the low-MW-aromatic compounds (low URI) were biodegraded during AD as discussed before (Fig. 2-b). In the case of the non-pre-treated samples, WAS and Blank samples, the fractions >29.1 kDa and ≤0.1 kDa decreased their specific aromaticity, indicated by an increased URI. The rest of the MW fractions increased their aromaticity after AD. Since WAS and Blank samples did not contain melanoidins, the changes in URI were most likely caused by changes in the EPS structure and the presence of degradation products of cell material in the case of WAS. The EPS spectrum has shown absorbance in the range 210–220 nm and 255–265 nm, which are related to protein and humic-like structures (Meng et al., 2016; Wang et al., 2018).

Fig. 2-d shows the NFRI corresponding to humic-like, fulvic-like and protein-like substances in the FEEM. As observed in Fig. 2-d NFRI decreased after AD showing a similar trend as sCOD (Fig. 1-a) and total area in SEC-HPLC analysis (Fig. 2-a and Fig. 2-b). Also, the pre-treated samples showed a higher degree of fluorescence compared to WAS, evidencing the presence of humic substances. Furthermore, it can be observed that after AD the humic-like and fulvic-like fractions remained at a similar level, indicating lower biodegradability in these fractions. On the other hand, the protein-like fraction decreased in all the samples after AD, indicating that this fraction can be degraded under anaerobic conditions. Overall, THP increased the solubilisation and formation of biodegradable and recalcitrant melanoidins. Among the aromatic compounds formed during THP, we observed anaerobic biodegradability in the low molecular weight fraction, which were associated with protein-like substances.

3.3. TAN formation and release

TAN release was studied in the fractionated substrates before and after AD. Despite that FAN is considered the main inhibitor, TAN was chosen as determining parameter since TAN can be measured directly, and it was not possible to differentiate the inhibition caused by NH_4^+ or FAN (Astals et al., 2018). Before AD, TAN originated from: TAN in the substrates, TAN present in the culture medium used in the BMP tests (Table A1), and TAN in the inoculum. Moreover, TAN release after the BMP tests originated from TAN released from substrate digestion, and TAN released from the inoculum due to endogenous respiration. Fig. 3 shows the concentration of TAN and soluble proteins, both before and after performing the BMP tests. The SDOSs of these compounds are shown in Fig. 3 as well. Following the former reasoning, we choose TAN-SDOSs and soluble proteins-SDOS to assess the TAN and soluble COD release caused exclusively by the substrates added in the BMP bottles.

From Fig. 3-a it can be observed that before AD, TAN-SDOSs of THP_l and THP_t showed values 3.5- and 1.7-times higher than WAS. The elevated TAN-SDOS concentration before AD indicated that the conditions during THP were such that they caused proteins deamination. The physicochemical breakdown of proteins to the extent of deamination during THP thermochemical reactions has already been reported by Wilson and Novak (2009). Conversely, before AD, TAN-SDOSs in WAS and THP_s showed the lowest values, indicating that in these samples, N was contained in the particulate organics. In addition to the TAN solubilisation/formation during pre-treatment, AD resulted in a TAN-SDOS increase of at least four times in all samples analysed.

Fig. 3-a and Fig. 3-b show that THP_l rendered the highest TAN-SDOS increase during AD showing that most of the biodegradable proteins were in the soluble fraction of THP-treated sludge. Strikingly, THP_s showed the lowest increase in TAN-SDOS during AD, i.e., from 2.8 to 19 $mgTAN/gCOD_{subs}$, indicating a lower concentration of biodegradable proteins in THP. Guo et al. (2020) showed the presence of structural proteins in WAS pellet being part of the non-soluble EPS matrix, which confirms our present finding. Fig. 3-b shows that the soluble proteins-SDOS before AD showed a similar tendency as TAN, rendering the highest values in the sample THP_l followed by THP_t. Fig. 3-b also shows that in all the cases the solubilised proteins are biodegradable during AD, which resulted in accumulating TAN in the digester broth.

The $TAN_{released}/COD_{consumed}$ ratios for the THP fractions were 99 ± 17, 46 ± 9 and 56 ± 15 mgTAN/gCOD in THP_l, THP_s and THP_t, and 64 ± 10 mgTAN/gCOD for WAS, respectively. Comparing $TAN_{released}/COD_{consumed}$, it can be inferred that THP_l consisted to a large extent of biodegradable proteins, considering 121 mgTAN/gCOD as the stoichiometric maximum from serum albumin digestion ($C_{123}H_{193}O_{37}N_{35}$, CAS 98420-25-8). The opposite was observed in THP_s, in which the biodegradable solid fraction released about half of the TAN that was released in total by THP_l during AD. The low $TAN_{released}/COD_{consumed}$ in THP_s indicated that the biodegradable solid fraction of THP_t contained less biodegradable proteins. Moreover, the THP_t sample released less TAN per biodegradable substrate than WAS. Considering that the BMP value of THP_t was higher than that of WAS, THP increased the biodegradability of other organics too (not just proteins). At the same time, the decrease in $TAN_{released}/COD_{consumed}$ in THP_t compared to WAS likely caused by the Maillard reaction, which rendered AD-recalcitrant melanoidins (Martins and van Boekel, 2003; Dwyer et al., 2008). Overall, THP increased the solubilisation of biodegradable organic matter (shown as THP_l) and increased the BMP and TAN release, specifically from the soluble fraction. However, the use of THP reduced the $TAN_{released}/COD_{consumed}$ ratio, due to the formation of melanoidins and deamination during THP (Wilson and Novak, 2009; Wilson et al., 2011).

3.4. Acute inhibition of the methanogenic biomass

By assessing the mSMA at the beginning of the BMP tests, using fresh inoculum and the fractionated substrates, we were able to determine any possible inhibitory effect on the methanogenic biomass caused by compounds that were present in the initial substrate, such as the organic matter released during pre-treatment. Additionally, the mSMA results obtained after the BMP tests (+AD) provided information about possible metabolites that were formed during AD, affecting the digestion process.

Fig. 4-a shows that the mSMAs of inoculum with the addition of the THP-pre-treated samples were 84.2 ± 1.3, 87.1 ± 1.7 and 87.0 ± 0.2 $mgCOD/gVS/day$ for THP_l, THP_s and THP_t respectively. Results showed that none of them was statistically different from the Blank sample (inoculum only), using mean differences *t*-test (p-values of 0.36, 0.08 and 0.1, respectively). The equal mSMA compared to the Blank in the pre-treated samples before BMP indicated that there was no (acute) inhibition of methanogens that could have been caused by compounds

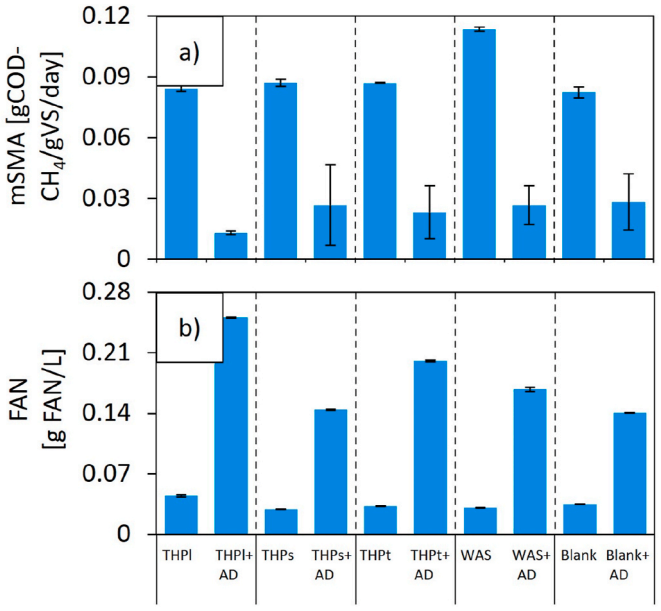

Fig. 4. a) mSMA before and after BMP tests (+AD) in all substrates; b) FAN concentration before and after BMP tests in all substrates.

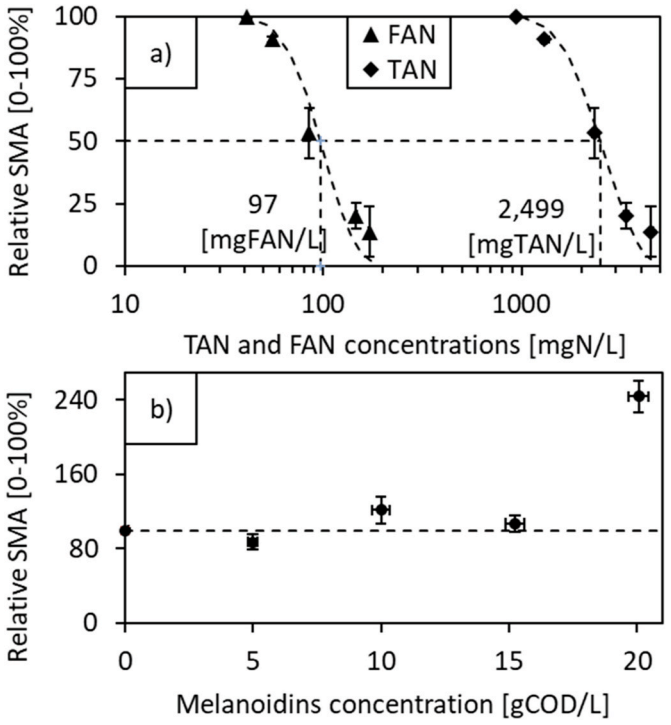

Fig. 5. a) Relative SMA values of the inoculum used in the mSMA and BMP tests at different concentrations TAN and FAN; 100% agrees with an SMA of 96 ± 1 mg COD/gVS/day. Note: X-axis is a log-scale. b) Relative SMA values at incremental melanoidins concentrations of the inoculum used in the SMA and BMP tests; 100% agrees with an SMA of 64 ± 1 mg COD/gVS/day.

formed or solubilised during THP. On the other hand, mSMA of WAS 39% higher compared to the blank test, which was significantly different with a p-value = 0.001 in a mean difference *t*-test. The difference in mSMA between the Blank and WAS addition might be explained by the storage of WAS in a "sludge-buffer-tank" at the WWTP for approximately two weeks. This storage period might have led to an accumulation of methanogenic microorganisms that increased the acetotrophic activity in this sample. The CAMBI® system at the WWTP was fed from the same sludge buffer, but any microbial activity would have been destroyed during the THP pre-treatment. Therefore, the mSMA in the samples with addition of the pre-treated fractions was not affected.

Fig. 4-a also shows the severe decrease in the microbial activity that was observed in all the samples analysed after the BMP tests (samples + AD). Results indicated that one or more compounds produced during AD decreased the acetotrophic activity of the anaerobic inoculum. The samples after AD were statistically indifferent with p-values of 0.628 in a single factor ANOVA, with 95% of confidence. Among the studied parameters, the increased concentrations of TAN and FAN possibly explained the decrease in acetotrophic activity after AD (Astals et al., 2018). Fig. 3-a and Fig. 4-b show the concentrations TAN and FAN, respectively, in the studied samples before and after the BMP tests. FAN increased in all the samples after AD, which was a consequence of the increased TAN concentration, plus a slight increase in the pH during the incubations. To the authors' knowledge, there is not a clear threshold in the literature for inhibition of acetotrophic methanogenic activity due to the presence of TAN and FAN (Capson-Tojo et al., 2020). Different authors reported different ranges of inhibition for TAN and FAN in AD, e.g. Bhattacharya and Parkin (1989) found that 55 mg FAN/L was the maximum tolerable concentration, while Calli et al. (2005) found a reduction in COD conversion in UASB reactors of 78–98%, with a concentration of 800 mgFAN/L. Literature results indicate that TAN and FAN inhibition thresholds, are inoculum-dependent and might vary depending on the operational conditions and acclimation of the microorganisms to these inhibitors (Chen et al., 2008; Lee et al., 2021; Moerland et al., 2021).

The influence of possible inhibitors in the samples was further assessed, using the same inoculum as in the mSMA test and applying incremental concentrations of TAN/FAN and melanoidins. Fig. 5-a and b show the relative SMA values as a percentage of the positive control (without inhibitor) at different TAN/FAN, and melanoidins concentrations. Both TAN and FAN distinctly decreased the SMAs (Fig. 5-a), and SMAs halved their maximum values at about 2.5 g TAN/L and 100 mg FAN/L. These half-inhibition concentrations were within the range that was observed in the studied samples after BMP (+AD). Moreover, the inoculum that was used in both (m)SMA and BMP was likely not well acclimated to increased concentrations of TAN and FAN, since the full-scale digester from where the inoculum was obtained contained around 789 mgTAN/L and 41 mgFAN/L. The mentioned full-scale digester was not equipped with any sludge pre-treatment technique.

Contrary to the observed TAN and FAN inhibition of the SMA, the SMAs at incremental concentrations of melanoidins showed no evidence of inhibition of the methanogenic activity, even at COD concentrations as high as 20 gCOD/L, when, conversely, higher activity was observed (Fig. 5-b). The increased activity can possibly be attributed to some methanogens that might have been contained in the melanoidins stock solution due to the anaerobic pre-digestion process with anaerobic digestate. Our current findings agree with the results of Rodríguez-Abalde et al. (2011) who did not find evidence that melanoidins can cause inhibition on methanogens. In contrast, Penaud et al. (2000) posed that there are recalcitrant compounds that may cause a decrease in anaerobic activity. However, in their study, TAN/FAN were not measured, although both compounds are expected to be present in ranges that might have led to process inhibition. Other studies also reported inhibition of methanogens by humic substances; however, the diversity of the microorganisms present in a full-scale inoculum might have helped to mitigate this effect (Khadem et al., 2017; Yap et al., 2018; Zhang et al., 2022). TAN/FAN are well-known inhibitors of AD. However, in literature, it is well described that anaerobic biomass can be acclimated to high TAN/FAN concentrations (Yan et al., 2019). The expected effect of increased TAN/FAN is especially high during the transition phase, when an AD reactor with no pre-treatment starts using THP. Under such conditions, the sudden increase in TAN/FAN concentrations might lead

to instabilities in the process before the anaerobic biomass is acclimated to the new regime.

4. Conclusions

From our present study the following conclusions can be drawn.

- THP of WAS released digestible organics and increased the concentration of aromatic compounds, which were partially biodegradable under anaerobic conditions. Especially, the aromatic fractions with a MW under 1.1 kDa that were related to protein-like compounds were partially biodegradable.
- TAN was limitedly released during THP solely, but TAN concentrations increased drastically during subsequent AD.
- THP increased the solubilisation and biodegradability of organic matter which increased the BMPs. However, the ratio $TAN_{released}$/$COD_{consumed}$ decreased, due to THP-related deamination and the Maillard reaction of proteinaceous material that forms partially AD-recalcitrant melanoidins.
- Melanoidins that were formed during THP of WAS did not cause acute inhibition on acetotrophic methanogenesis of a full-scale inoculum sample.
- Inhibition of methanogens, while digesting THP-treated sludge, was likely a consequence of the released TAN (and FAN formation) from an increased amount of biodegradable proteins.

Credit author statement

Javier Pavez-Jara: Conceptualization, Methodology, Formal analysis, Investigation, Resources, Data curation, Writing – original draft. Merle de Kreuk: Resources, Writing – review & editing, Visualization, Supervision, Project administration, Funding acquisition. Jules van Lier: Resources, Writing – review & editing, Visualization, Supervision, Project administration, Funding acquisition.

Funding source disclosure

This work was funded by ANID PFCHA/DOCEXT 72170548, TU Delft, STOWA, Paques BV, and Water Authorities from the Netherlands (Waterschap de Dommel, Waterschap Vechtstromen, Waterschap Vallei en Veluwe and Waterschap Limburg). This activity is co-financed by the Surcharge for Topconsortia for Knowledge and Innovation (TKI) of the Ministry of Economic Affairs, The Netherlands.

Submission declaration

The authors declare that this work has not been published previously and that it is not under consideration for publication elsewhere. The publication is approved by all authors and by the responsible authorities where the work was carried out, and that, if accepted, it will not be published elsewhere including electronically in the same form, in English or in any other language, without the written consent of the copyright-holder.

Declaration of competing interest

The authors declare that they have no known competing financial interests or personal relationships that could have appeared to influence the work reported in this paper.

Data availability

Data will be made available on request.

Acknowledgement

This work was funded by ANID PFCHA/DOCEXT 72170548, TU Delft, STOWA, Paques BV, and Water Authorities from the Netherlands (Waterschap de Dommel, Waterschap Vechtstromen, WaterschapVallei en Veluwe and Waterschap Limburg). This activity is co-financed by the Surcharge for Topconsortia for Knowledge and Innovation (TKI) of the Ministry of Economic Affairs, The Netherlands. The authors want to thank the operators of Harnaschpolder and Hengelo wastewater treatment plants for their kind contribution in providing the samples to carry out this work.

Appendix A. Supplementary data

Supplementary data to this article can be found online at https://doi.org/10.1016/j.chemosphere.2023.138896.

References

Akindele, A.A., Sartaj, M., 2018. The toxicity effects of ammonia on anaerobic digestion of organic fraction of municipal solid waste. Waste Manag. 71, 757–766.
Appels, L., Baeyens, J., Degrève, J., Dewil, R., 2008. Principles and potential of the anaerobic digestion of waste-activated sludge. Prog. Energy Combust. Sci. 34, 755–781.
Astals, S., Peces, M., Batstone, D.J., Jensen, P.D., Tait, S., 2018. Characterising and modelling free ammonia and ammonium inhibition in anaerobic systems. Water Res. 143, 127–135.
Balasundaram, G., Banu, R., Varjani, S., Kazmi, A.A., Tyagi, V.K., 2022. Recalcitrant compounds formation, their toxicity, and mitigation: key issues in biomass pretreatment and anaerobic digestion. Chemosphere 291, 132930.
Barber, W.P.F., 2016. Thermal hydrolysis for sewage treatment: a critical review. Water Res. 104, 53–71.
Bernardo, E.C., Egashira, R., Kawasaki, J., 1997. Decolorization of molasses' wastewater using activated carbon prepared from cane bagasse. Carbon 35, 1217–1221.
Bhattacharya, S.K., Parkin, G.F., 1989. The effect of ammonia on methane fermentation processes. J. Water Pollut. Control Federation 55–59.
Boopathy, R., 2002. Methanogenesis from furfural by defined mixed cultures. Curr. Microbiol. 44, 406–410.
Brons, H.J., Field, J.A., Lexmond, W.A.C., Lettinga, G., 1985. Influence of humic acids on the hydrolysis of potato protein during anaerobic digestion. Agric. Wastes 13, 105–114.
Calli, B., Mertoglu, B., Inanc, B., Yenigun, O., 2005. Effects of high free ammonia concentrations on the performances of anaerobic bioreactors. Process Biochem. 40, 1285–1292.
Capson-Tojo, G., Moscoviz, R., Astals, S., Robles, Á., Steyer, J.P., 2020. Unraveling the literature chaos around free ammonia inhibition in anaerobic digestion. Renew. Sustain. Energy Rev. 117, 109487.
Chandra, R., Bharagava, R.N., Rai, V., 2008. Melanoidins as major colourant in sugarcane molasses based distillery effluent and its degradation. Bioresour. Technol. 99, 4648–4660.
Chen, W., Westerhoff, P., Leenheer, J.A., Booksh, K., 2003. Fluorescence Excitation−Emission matrix regional integration to quantify spectra for dissolved organic matter. Environ. Sci. Technol. 37, 5701–5710.
Chen, Y., Cheng, J.J., Creamer, K.S., 2008. Inhibition of anaerobic digestion process: a review. Bioresour. Technol. 99, 4044–4064.
D'Abzac, P., Bordas, F., Van Hullebusch, E., Lens, P.N.L., Guibaud, G., 2010. Extraction of extracellular polymeric substances (EPS) from anaerobic granular sludges: comparison of chemical and physical extraction protocols. Appl. Microbiol. Biotechnol. 85, 1589–1599.
Deng, Z., van Linden, N., Guillen, E., Spanjers, H., van Lier, J.B., 2021. Recovery and applications of ammoniacal nitrogen from nitrogen-loaded residual streams: a review. J. Environ. Manag. 295, 113096.
Dubois, M., Gilles, K., Hamilton, J.K., Rebers, P.A., Smith, F., 1951. A colorimetric method for the determination of sugars. Nature 168, 167-167.
Dwyer, J., Lant, P., 2008. Biodegradability of DOC and DON for UV/H2O2 pre-treated melanoidin based wastewater. Biochem. Eng. J. 42, 47–54.
Dwyer, J., Starrenburg, D., Tait, S., Barr, K., Batstone, D.J., Lant, P., 2008. Decreasing activated sludge thermal hydrolysis temperature reduces product colour, without decreasing degradability. Water Res. 42, 4699–4709.
Ellis, G.P., 1959. The maillard reaction. In: Wolfrom, M.L. (Ed.), Advances in Carbohydrate Chemistry. Academic Press, pp. 63–134.
Emerson, K., Russo, R.C., Lund, R.E., Thurston, R.V., 1975. Aqueous ammonia equilibrium calculations: effect of pH and temperature. J. Fisheries Board. Canada 32, 2379–2383.
Fr, B., Griebe, T., Nielsen, P., 1995. Enzymatic activity in the activated-sludge floc matrix. Appl. Microbiol. Biotechnol. 43, 755–761.
Fux, C., Siegrist, H., 2004. Nitrogen removal from sludge digester liquids by nitrification/denitrification or partial nitritation/anammox: environmental and economical considerations. Water Sci. Technol. 50, 19–26.

Fytili, D., Zabaniotou, A., 2008. Utilization of sewage sludge in EU application of old and new methods—a review. Renew. Sustain. Energy Rev. 12, 116–140.
Gao, J., Li, L., Yuan, S., Chen, S., Dong, B., 2022. The neglected effects of polysaccharide transformation on sludge humification during anaerobic digestion with thermal hydrolysis pretreatment. Water Res. 226, 119249.
Gonzalez, A., Hendriks, A.T.W.M., van Lier, J.B., de Kreuk, M., 2018. Pre-treatments to enhance the biodegradability of waste activated sludge: elucidating the rate limiting step. Biotechnol. Adv. 36, 1434–1469.
Guo, H., Felz, S., Lin, Y., van Lier, J.B., de Kreuk, M., 2020. Structural extracellular polymeric substances determine the difference in digestibility between waste activated sludge and aerobic granules. Water Res. 181, 115924.
Haug, R.T., Stuckey, D.C., Gossett, J.M., McCarty, P.L., 1978. Effect of thermal pretreatment on digestibility and dewaterability of organic sludges. J. Water Pollu. Control Federation 73–85.
Her, N., Amy, G., Sohn, J., Gunten, U., 2008. UV absorbance ratio index with size exclusion chromatography (URI-SEC) as an NOM property indicator. J. Water Supply Res. Technol. - Aqua 57, 35–44.
Higgins, M.J., Beightol, S., Mandahar, U., Suzuki, R., Xiao, S., Lu, H.-W., Le, T., Mah, J., Pathak, B., DeClippeleir, H., Novak, J.T., Al-Omari, A., Murthy, S.N., 2017. Pretreatment of a primary and secondary sludge blend at different thermal hydrolysis temperatures: impacts on anaerobic digestion, dewatering and filtrate characteristics. Water Res. 122, 557–569.
Hodge, J.E., 1953. Dehydrated foods, chemistry of browning reactions in model systems. J. Agric. Food Chem. 1, 928–943.
Holliger, C., Alves, M., Andrade, D., Angelidaki, I., Astals, S., Baier, U., Bougrier, C., Buffière, P., Carballa, M., De Wilde, V., 2016. Towards a standardization of biomethane potential tests. Water Sci. Technol., wst2016336
Horvat, Š., Jakas, A., 2004. Peptide and amino acid glycation: new insights into the maillard reaction. J. Pept. Sci. 10, 119–137.
Huang, C., Xiong, L., Guo, H.-J., Li, H.-L., Wang, C., Chen, X.-F., Zhao, C., Chen, X.-D., 2019. Anaerobic digestion of elephant grass hydrolysate: biogas production, substrate metabolism and outlet effluent treatment. Bioresour. Technol. 283, 191–197.
Jeong, S.Y., Chang, S.W., Ngo, H.H., Guo, W., Nghiem, L.D., Banu, J.R., Jeon, B.-H., Nguyen, D.D., 2019. Influence of thermal hydrolysis pretreatment on physicochemical properties and anaerobic biodegradability of waste activated sludge with different solids content. Waste Manag. 85, 214–221.
Kabouris, J.C., Tezel, U., Pavlostathis, S.G., Engelmann, M., Dulaney, J., Gillette, R.A., Todd, A.C., 2009. Methane recovery from the anaerobic codigestion of municipal sludge and FOG. Bioresour. Technol. 100, 3701–3705.
Kelessidis, A., Stasinakis, A.S., 2012. Comparative study of the methods used for treatment and final disposal of sewage sludge in European countries. Waste Manag. 32, 1186–1195.
Kepp, U., Machenbach, I., Weisz, N., Solheim, O.E., 2000. Enhanced stabilisation of sewage sludge through thermal hydrolysis - three years of experience with full scale plant. Water Sci. Technol. 42, 89–96.
Khadem, A.F., Azman, S., Plugge, C.M., Zeeman, G., van Lier, J.B., Stams, A.J.M., 2017. Effect of humic acids on the activity of pure and mixed methanogenic cultures. Biomass Bioenergy 99, 21–30.
Klavins, M., Eglite, L., Serzane, J., 1999. Methods for analysis of aquatic humic substances. Crit. Rev. Anal. Chem. 29, 187–193.
Koster, I.W., Lettinga, G., 1984. The influence of ammonium-nitrogen on the specific activity of pelletized methanogenic sludge. Agric. Wastes 9, 205–216.
Lee, J., Kim, E., Hwang, S., 2021. Effects of inhibitions by sodium ion and ammonia and different inocula on acetate-utilizing methanogenesis: methanogenic activity and succession of methanogens. Bioresour. Technol. 334, 125202.
Li, J., Hao, X., van Loosdrecht, M.C.M., Luo, Y., Cao, D., 2019. Effect of humic acids on batch anaerobic digestion of excess sludge. Water Res. 155, 431–443.
Lin, J.-G., Chang, C.-N., Chang, S.-C., 1997. Enhancement of anaerobic digestion of waste activated sludge by alkaline solubilization. Bioresour. Technol. 62, 85–90.
Luostarinen, S., Luste, S., Sillanpää, M., 2009. Increased biogas production at wastewater treatment plants through co-digestion of sewage sludge with grease trap sludge from a meat processing plant. Bioresour. Technol. 100, 79–85.
MacCarthy, P., 2001. The principles of humic substances. Soil Sci. 166, 738–751.
Martins, S.I.F.S., van Boekel, M.A.J.S., 2003. Melanoidins extinction coefficient in the glucose/glycine Maillard reaction. Food Chem. 83, 135–142.
Mata-Alvarez, J., Dosta, J., Romero-Güiza, M.S., Fonoll, X., Peces, M., Astals, S., 2014. A critical review on anaerobic co-digestion achievements between 2010 and 2013. Renew. Sustain. Energy Rev. 36, 412–427.
Meng, L., Xi, J., Yeung, M., 2016. Degradation of extracellular polymeric substances (EPS) extracted from activated sludge by low-concentration ozonation. Chemosphere 147, 248–255.
Migo, V.P., Matsumura, M., Del Rosario, E.J., Kataoka, H., 1993. The effect of pH and calcium ions on the destabilization of melanoidin. J. Ferment. Bioeng. 76, 29–32.
Moerland, M.J., Bruning, H., Buisman, C.J.N., van Eekert, M.H.A., 2021. Advanced modelling to determine free ammonia concentrations during (hyper-)thermophilic anaerobic digestion in high strength wastewaters. J. Environ. Chem. Eng. 9, 106724.
Ngo, P.L., Udugama, I.A., Gernaey, K.V., Young, B.R., Baroutian, S., 2021. Mechanisms, status, and challenges of thermal hydrolysis and advanced thermal hydrolysis processes in sewage sludge treatment. Chemosphere 281, 130890.
Ochs, P., Martin, B., Germain-Cripps, E., Stephenson, T., van Loosdrecht, M., Soares, A., 2023. Techno-economic analysis of sidestream ammonia removal technologies: biological options versus thermal stripping. Environ. Sci. Ecotechnol. 13, 100220.
Ohemeng-Ntiamoah, J., Datta, T., 2018. Evaluating analytical methods for the characterization of lipids, proteins and carbohydrates in organic substrates for anaerobic co-digestion. Bioresour. Technol. 247, 697–704.
Ortega-Martínez, E., Chamy, R., Jeison, D., 2021. Thermal pre-treatment: getting some insights on the formation of recalcitrant compounds and their effects on anaerobic digestion. J. Environ. Manag. 282, 111940.
Park, J.-H., Yoon, J.-J., Park, H.-D., Lim, D.J., Kim, S.-H., 2012. Anaerobic digestibility of algal bioethanol residue. Bioresour. Technol. 113, 78–82.
Penaud, V., Delgenès, J.-P., Moletta, R., 2000. Characterization of soluble molecules from thermochemically pretreated sludge. J. Environ. Eng. 126, 397–402.
Pérez-Elvira, S., Fdz-Polanco, M., Fdz-Polanco, F., 2010. Increasing the performance of anaerobic digestion: pilot scale experimental study for thermal hydrolysis of mixed sludge. Front. Environ. Sci. Eng. China 4, 135–141.
Rahmani, A.M., Tyagi, V.K., Gunjyal, N., Kazmi, A.A., Ojha, C.S.P., Moustakas, K., 2023. Hydrothermal and thermal-alkali pretreatments of wheat straw: Co-digestion, substrate solubilization, biogas yield and kinetic study. Environ. Res. 216, 114436.
Rice, E.W., Baird, R.B., Eaton, A.D., Clesceri, L.S., 2012. Standard Methods for the Examination of Water and Wastewater. American Public Health Association, Washington, DC.
Ringoot, D., Kleiven, H., Panter, K., 2012. Energy Efficient Thermal Hydrolysis with Steam Explosion. 17th European Biosolids and Organic Resources Conference Abstract, pp. 1–8.
Rodríguez-Abalde, Á., Fernández, B., Silvestre, G., Flotats, X., 2011. Effects of thermal pre-treatments on solid slaughterhouse waste methane potential. Waste Manag. 31, 1488–1493.
Rufian-Henares, J.A., de la Cueva, S.P., 2009. Antimicrobial activity of coffee Melanoidins. A study of their metal-chelating properties. J. Agric. Food Chem. 57, 432–438.
Silván, J.M., van de Lagemaat, J., Olano, A., del Castillo, M.D., 2006. Analysis and biological properties of amino acid derivates formed by Maillard reaction in foods. J. Pharmaceut. Biomed. Anal. 41, 1543–1551.
Squire, P.G., 1985. [10] Hydrodynamic Characterization of Random Coil Polymers by Size Exclusion Chromatography. Methods in Enzymology. Academic Press, pp. 142–153.
Stuckey, D.C., McCarty, P.L., 1984. The effect of thermal pretreatment on the anaerobic biodegradability and toxicity of waste activated sludge. Water Res. 18, 1343–1353.
Suárez-Iglesias, O., Urrea, J.L., Oulego, P., Collado, S., Díaz, M., 2017. Valuable compounds from sewage sludge by thermal hydrolysis and wet oxidation. A review. Sci. Total Environ. 584–585, 921–934.
Sutton, R., Sposito, G., 2005. Molecular structure in soil humic substances: the new view. Environ. Sci. Technol. 39, 9009–9015.
Tarvers, R.C., Church, F.C., 1985. Use of high-performance size-exclusion chromatography to measure protein molecular weight and hydrodynamic radius. An investigation of the properties of the TSK 3000 SW column. Int. J. Pept. Protein Res. 26, 539–549.
Valo, A., Carrère, H., Delgenès, J.P., 2004. Thermal, chemical and thermo-chemical pre-treatment of waste activated sludge for anaerobic digestion. J. Appl. Chem. Biotechnol. 79, 1197–1203.
Vineyard, D., Hicks, A., Karthikeyan, K.G., Barak, P., 2020. Economic analysis of electrodialysis, denitrification, and anammox for nitrogen removal in municipal wastewater treatment. J. Clean. Prod. 262, 121145.
Wang, B.-B., Liu, X.-T., Chen, J.-M., Peng, D.-C., He, F., 2018. Composition and functional group characterization of extracellular polymeric substances (EPS) in activated sludge: the impacts of polymerization degree of proteinaceous substrates. Water Res. 129, 133–142.
Wang, S., Hu, Z.-Y., Geng, Z.-Q., Tian, Y.-C., Ji, W.-X., Li, W.-T., Dai, K., Zeng, R.J., Zhang, F., 2022. Elucidating the production and inhibition of melanoidins products on anaerobic digestion after thermal-alkaline pretreatment. J. Hazard Mater. 424, 127377.
Wilén, B.-M., Jin, B., Lant, P., 2003. The influence of key chemical constituents in activated sludge on surface and flocculating properties. Water Res. 37, 2127–2139.
Wilson, C.A., Novak, J.T., 2009. Hydrolysis of macromolecular components of primary and secondary wastewater sludge by thermal hydrolytic pretreatment. Water Res. 43, 4489–4498.
Wilson, C.A., Tanneru, C.T., Banjade, S., Murthy, S.N., Novak, J.T., 2011. Anaerobic digestion of raw and thermally hydrolyzed wastewater solids under various operational conditions. Water Environ. Res. 83, 815–825.
Yan, M., Fotidis, I.A., Tian, H., Khoshnevisan, B., Treu, L., Tsapekos, P., Angelidaki, I., 2019. Acclimatization contributes to stable anaerobic digestion of organic fraction of municipal solid waste under extreme ammonia levels: focusing on microbial community dynamics. Bioresour. Technol. 286, 121376.
Yang, G., Zhang, G., Wang, H., 2015. Current state of sludge production, management, treatment and disposal in China. Water Res. 78, 60–73.
Yap, S.D., Astals, S., Lu, Y., Peces, M., Jensen, P.D., Batstone, D.J., Tait, S., 2018. Humic acid inhibition of hydrolysis and methanogenesis with different anaerobic inocula. Waste Manag. 80, 130–136.
Yin, J., Liu, J., Chen, T., Long, Y., Shen, D., 2019. Influence of melanoidins on acidogenic fermentation of food waste to produce volatility fatty acids. Bioresour. Technol. 284, 121–127.
Zhang, L., Gong, X., Xu, R., Guo, K., Wang, L., Zhou, Y., 2022. Responses of mesophilic anaerobic sludge microbiota to thermophilic conditions: implications for start-up and operation of thermophilic THP-AD systems. Water Res. 216, 118332.
Zhen, G., Lu, X., Kato, H., Zhao, Y., Li, Y.-Y., 2017. Overview of pretreatment strategies for enhancing sewage sludge disintegration and subsequent anaerobic digestion: current advances, full-scale application and future perspectives. Renew. Sustain. Energy Rev. 69, 559–577.